

# Effects of thermal cycling and thermal aging on the hermeticity and strength of silver–copper oxide air-brazed seals<sup>☆</sup>

K. Scott Weil<sup>a,\*</sup>, Christopher A. Coyle<sup>a</sup>, Jens T. Darsell<sup>b</sup>, Gordon G. Xia<sup>c</sup>, John S. Hardy<sup>a</sup>

<sup>a</sup> Energy Science and Technology Division, Pacific Northwest National Laboratory, Richland, WA 99352, USA

<sup>b</sup> School of Mechanical and Materials Engineering, Washington State University, Pullman, WA 99164, USA

<sup>c</sup> Environmental Technology Division, Pacific Northwest National Laboratory, Richland, WA 99352, USA

Received 18 December 2004; accepted 12 January 2005

Available online 23 March 2005

## Abstract

Thermal cycle and exposure tests were conducted on ceramic-to-metal joints prepared by a new sealing technique. Known as reactive air brazing, this joining method is currently being considered for use in sealing various high-temperature solid-state electrochemical devices, including planar solid oxide fuel cells (pSOFC). In order to simulate a typical pSOFC application, test specimens were prepared by joining ceramic anode/electrolyte bilayers to metal washers, of the same composition as the common frame materials employed in pSOFC stacks, using a filler metal composed of 4 mol% CuO in silver. The brazed samples were exposure tested at 750 °C for 200, 400, and 800 h in both simulated fuel and air environments and thermally cycled at rapid rate (75 °C min<sup>-1</sup>) between room temperature and 750 °C for as many as 50 cycles. Subsequent joint strength testing and microstructural analysis indicated that the samples exposure tested in air displayed little degradation with respect to strength, hermeticity, or microstructure out to 800 h of exposure. Those tested in fuel showed no change in rupture strength or loss in hermeticity after 800 h of high-temperature exposure, but did undergo microstructural change due to the dissolution of hydrogen into the silver-based braze material. Air-brazed specimens subjected to rapid thermal cycling exhibited no loss in joint strength or hermeticity, but displayed initial signs of seal delamination along the braze–electrolyte interface after 50 cycles.

Published by Elsevier B.V.

**Keywords:** Thermal cycling; Silver–copper oxide; Hermeticity

## 1. Introduction

Among the SOFC designs currently under development at various organizations, the planar stack configuration (pSOFC) has received growing attention because its compact construction affords high volumetric power density—a design feature of particular importance in transportation applications. With the advent of anode-supported cells that employ thin YSZ electrolytes, these devices can be operated at reduced temperature (700–800 °C) and still achieve the same current densities exhibited by their high-temperature, thick electrolyte-supported counterparts [1]. The lower

operating temperature not only makes it possible to consider inexpensive, commercially available high-temperature alloys for use in the stack and balance of plant, but also expands the list of materials that could be employed in device sealing [2].

Because SOFCs function under an oxygen ion gradient that develops across the electrolyte, hermeticity across this membrane is paramount. In a planar design, this means that not only must the YSZ electrolyte layer be dense, i.e. contain no interconnected porosity, but that it must also be connected to the rest of the device with a high temperature, gas-tight seal. One of the fundamental challenges in fabricating pSOFCs is how to effectively join the thin, electrochemically active ceramic membrane to the metallic body of the device such that the resulting seal remains hermetic, rugged, and stable during continuous high-temperature, long-term use. Typical pSOFC operating conditions assumed in the present study include: (1) an average operating temperature of 750 °C; (2)

<sup>☆</sup> This paper was presented at the 2004 Fuel Cell Seminar, San Antonio, TX, USA.

\* Corresponding author. Tel.: +1 509 375 6796; fax: +1 509 375 4448.

E-mail address: [scott.weil@pnl.gov](mailto:scott.weil@pnl.gov) (K. Scott Weil).

continuous exposure to an oxidizing atmosphere (air) on the cathode side and a wet reducing gas ( $\text{H}_2$  containing  $\sim 3\%$   $\text{H}_2\text{O}$ ) on the anode side; and (3) an anticipated device lifetime of 10,000+ h.

While a number of sealing techniques [3–10] are under consideration for pSOFC stack design, including glass bonding [3–5], compressive sealing [6–8], and reactive joining [9,10], one of the most reliable and best understood methods of joining dissimilar materials is brazing [11–13]. In this technique, a filler metal with a liquidus well below that of the materials to be joined is heated to a point at which it becomes molten and under capillary action fills the gap between the two pieces. Upon cooling, a solid joint forms. When applied to the bonding of ceramics, it has been found that the addition of a reactive metal is required, such as Ti or Zr (known as active metal brazing), to cause reduction of the ceramic at the joining interface and thereby create an intermediate layer that is in chemical equilibrium with both the underlying ceramic and the molten braze filler metal [14]. This chemically reduced surface is then readily wetted by the remaining braze material [15].

However, active metal brazing requires a stringent firing atmosphere, either high vacuum or reducing-gas conditions, to prevent the active species from pre-oxidizing. This represents higher capital and operating costs relative to air-fired processes such as glass bonding. In addition, it has been observed that exposure of the device to a reducing atmosphere at a temperature greater than  $\sim 800^\circ\text{C}$ , typical processing conditions employed in active metal brazing, may be too demanding for the complex oxide materials used in the ceramic cell and adjacent components. For example, many of the mixed ionic/electronic conducting perovskites under consideration for use in the cathode layer will reduce under these heat treatment conditions and may undergo irreversible deterioration via phase separation, causing severe degradation in stack performance.

To prevent these problems, we have recently developed a method of ceramic-to-metal brazing specifically for use in fabricating high-temperature solid-state devices such as pSOFCs and oxygen and hydrogen concentrators [16]. Referred to as air brazing, the technique differs from traditional ceramic brazing in two important ways: (1) it utilizes a liquid-phase oxide/noble metal melt as the basis for joining, and thereby exhibits inherent high-temperature oxidation resistance, and (2) the process can be conducted directly in air without the use of fluxes and/or inert cover gases. In fact, the strength of the bond formed during air brazing relies on the formation of a thin, adherent oxide scale on the metal substrate. One system that has shown particular promise in the development of air brazing is Ag–CuO. Prior work has shown that the addition of 1.4–8 mol% CuO to silver results in excellent wetting on a variety of oxide surfaces, while producing filler metal and interfacial microstructures that lead to good joint strength [16–18]. In the present study, the effects of thermal aging under prototypical pSOFC fuel and oxidant atmospheres and of aggressive thermal cycling on the subse-

quent rupture strength and microstructure of air-brazed seals are considered. In part, our interest is in identifying potential degradation mechanisms in these joints when exposed to the type of pSOFC operating conditions that might be expected in a transportation application [19,20].

## 2. Experimental

### 2.1. Materials

As shown in Fig. 1, a miniaturized version of the cell-to-frame component is the key test specimen employed in this study. Each sample was prepared by brazing a 25 mm diameter ceramic bilayer directly to a Crofer-22 APU washer that measures 44 mm in outside diameter with a 15 mm diameter concentric hole. The bilayer coupons are composed of a thick NiO–5YSZ anode layer co-sintered to a thin 5YSZ electrolyte, each of which was fabricated by a tape casting procedure that is identical to that used in fabricating full-scale, anode-supported pSOFC cells [21]. The anode layer was prepared by ball milling a 38:25:37 volume percent ratio of NiO (J.T. Baker, Inc.), 5YSZ (Zirconia Sales, Inc.), and carbon black (Columbia Inc.) powders with a proprietary binder and dispersant system in 2-butanone/ethyl alcohol for 1.5 days. The resulting slurry was cast onto silicone-coated mylar by the doctor blade technique, forming a  $\sim 0.4$  mm thick tape after solvent evaporation. Similarly, electrolyte tapes were fabricated by ball milling 5YSZ in the same solvent system for 2 days, followed by doctor blade casting and air drying to form tapes with a final thickness of approximately  $50\ \mu\text{m}$ . Both sets of tape were then laser cut into  $100\ \text{mm} \times 100\ \text{mm}$  plies. Multiple plies of the anode tape were laminated with a single ply of the electrolyte tape at  $70^\circ\text{C}$  and 250 psi for 45 s to form a single green bilayer tape. Discs measuring 30 mm in diameter were laser cut from this material and sintered in air at  $1350^\circ\text{C}$  for 1 h, yielding finished bilayer coupons measuring nominally 25 mm in diameter by  $600\ \mu\text{m}$  in thickness, with an average electrolyte thickness of  $\sim 8\ \mu\text{m}$ . In several series of tests, thicker bilayers were employed measuring  $\sim 1200\ \mu\text{m}$  in thickness. These were fabricated in a similar manner by laminating twice as many plies of anode tape.

The metal washers were fabricated from Crofer-22 APU (23% Cr, 0.45% Mn, 0.08% Ti, 0.06% La, bal. Fe). This alloy was chosen because: (1) it is a low-cost, ferritic stainless steel material of the type currently under consideration by a number of pSOFC stack manufacturers, (2) it forms a protective oxide scale that offers good oxidation resistance properties at  $700$ – $800^\circ\text{C}$ , and (3) its coefficient of thermal expansion (CTE) closely matches that of the NiO–YSZ/YSZ bilayer. Flat washer-shaped specimens were cut from  $300\ \mu\text{m}$  thick sheet via electrical discharge machining. The sealing surface of each was left in the as-received rolled condition, but was degreased ultrasonically in acetone for 10 min and wiped with methanol prior to use.

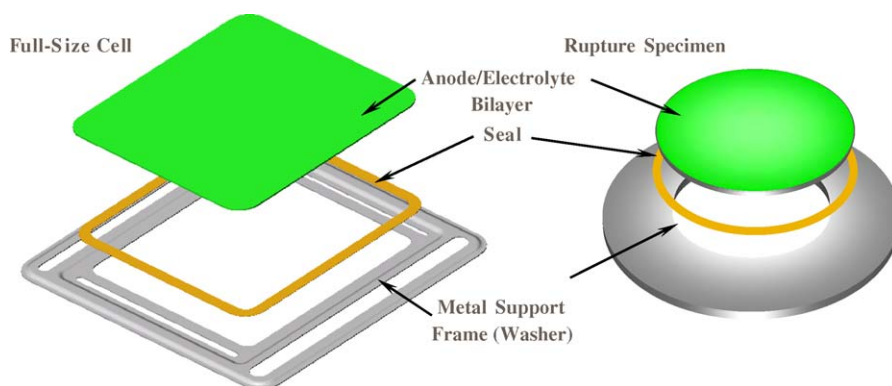


Fig. 1. Comparison of the full-size SOFC window frame component to the rupture test specimen (not shown to scale)

The filler material used in brazing was formulated by ball milling in methanol the appropriate amounts of copper (99%, Alfa Aesar) and silver powder (99.9%, Alfa Aesar) required to achieve an as-oxidized target composition of 4 mol% CuO in silver. Previous results from X-ray diffraction indicate that the copper powder will fully oxidize in situ during a typical air brazing heating schedule to form CuO, the wetting agent employed in this method of air brazing [22]. The milled powder was dried, then mixed with a polymer binder (B75717, Ferro Corp.) in a 1:1 weight ratio to form a paste that could be dispensed onto the substrate surfaces at a uniform rate of  $0.1 \text{ g (linear cm)}^{-1}$  using an automated syringe dispenser. In this manner, the filler metal paste was dispensed onto the YSZ side of the bilayer discs. Each disc was concentrically positioned on a washer specimen, loaded with a 100 g weight, and heated in air under the following brazing schedule: heat from room temperature to  $1000 \text{ }^\circ\text{C}$  at  $10 \text{ }^\circ\text{C min}^{-1}$ , hold at  $1000 \text{ }^\circ\text{C}$  for 15 min, and cool to room temperature at  $5 \text{ }^\circ\text{C min}^{-1}$ .

## 2.2. Testing and characterization

The potential methods by which a rigid pSOFC seal can fail during operation have been previously reviewed [23]. These include: (1) failure by fracture due to over-pressurization, (2) failure during rapid thermal cycling or due to thermal cycle fatigue, and (3) failure upon thermal aging. Externally induced mechanical shock can also be added to this list for consideration in transportation applications. A semi-quantitative mechanical test, the rupture test, has recently been developed specifically for the purpose of screening the vast number of material, processing, and operational parameters that may impact the efficacy of a given pSOFC sealing technique [23]. Essentially a modified version of an adhesive blister testing technique [24], the test was employed in the present study to investigate the possible degradation of air-brazed seals that have undergone rapid thermal cycling and/or thermal aging. It is conducted by placing a sealed disk specimen in a test fixture and slowly pressurizing the backside of the sample until seal rupture occurs, which gives a measure of the maximum pressure that the specimen can withstand. That is, the specimen is subjected to an accelerated stress test,

using air pressure to generate high levels of stress within the seal. Alternatively, a digital regulator used in testing allows the pressure behind the test specimen to be slowly increased to a given sub-critical set point. This volume of compressed gas ( $\sim 40 \text{ ml}$ ) can be isolated between the specimen and an external valve, making it possible to identify a leak in the seal by a decay in pressure. In this way, the device can be used to measure the hermeticity of a given seal configuration without causing destructive failure in the seal. A maximum pressure of 130 psi and a minimum of six specimens for each joining condition were employed in testing. Specific details concerning the design of the test apparatus and the testing procedure have been previously reported [23].

It is important to recognize that the differential pressure expected to arise across each individual cell in an actual operating stack is quite small; i.e. except under an accidental transient condition, the first failure mechanism listed above is unlikely. Thus in actuality, the rupture strength test places the cell, seal, and metal frame under a highly exaggerated stress condition relative to prototypic steady-state operation. However by doing so, the test makes it possible to identify the weakest constituent in the sealing system, i.e. the ceramic substrate, the braze material, the metal substrate and associated oxide scale, or any of the interfaces in between, so that the seal can potentially be improved in the next round of development. Ideally for the purposes of quantitative comparison, one would like the stress in the seal to be either pure shear or pure tension at failure. Unfortunately, the stress state in the rupture test specimen is mixed-mode. Although the test does not yield a strict quantitative measure of failure stress in the seal, it does provide a figure of merit, rupture stress, which can be used in comparing batches of specimens that have been joined or tested under alternate conditions.

One hundred and twenty air-brazed specimens were initially tested for hermeticity by pressurizing to 20 psi, closing the isolation valve, and examining the rate of pressure decay over a period of 10 min. Samples that displayed no decay, over 98% of those tested, were subsequently used in evaluating the thermal aging and cycling properties of the brazed seals. A representative baseline rupture strength was established by testing 12 of the specimens in the as-brazed

condition. Aging tests were then conducted by exposing sets of six specimens at 750 °C to either 20 cm<sup>3</sup> min<sup>-1</sup> of flowing dry air or 10 cm<sup>3</sup> min<sup>-1</sup> of commercially pure hydrogen bubbled through room temperature water for 200, 400, or 800 h. Upon cooling, the specimens were tested for hermeticity as described above, then pressurized to failure.

Thermal cycle testing was conducted in a pancake-shaped infrared furnace containing a horizontal 3 in. thick × 15 in. diameter chamber that was lined on top and bottom with quartz windows through which a series of high-intensity quartz lamps could radiate and thereby induce rapid rates of heating with great reproducibility. The specimens were heated to 750 °C at 75 °C min<sup>-1</sup> and held at temperature for 10 min followed by cooling at 75 °C min<sup>-1</sup> to 400 °C, after which the samples were cooled to 70 °C in approximately 25 min. Testing was generally conducted in dry flowing air (20 cm<sup>3</sup> min<sup>-1</sup>; although as will be discussed, several tests were conducted using dry Ar + 2.75% H<sub>2</sub>) out to a total of 5, 10, 20 or 50 cycles, after which the samples were tested for hermeticity and rupture strength. Microstructural analysis of the joints after rupture testing was conducted on polished cross-sectioned samples using a JEOL JSM-5900LV scanning electron microscope (SEM) equipped with an Oxford energy dispersive X-ray analysis (EDX) system. In order to avoid electrical charging on the samples, they were carbon coated and grounded. Elemental profiles were determined across the joint interfaces in the line-scan mode.

### 3. Results and discussion

#### 3.1. Effects of thermal aging

Plotted in Fig. 2(a) and (b) are the average leak rates and rupture strengths of the brazed sealing specimens, exposed respectively in air and wet hydrogen, as a function of time at 750 °C. The results suggest that thermal aging in either atmosphere has no significant effect on hermeticity and little effect on joint strength out to 800 h. Regardless of the atmosphere in which they were aged, all of the specimens appeared to fail in the same manner, due to fracture initiating within the cell. Examples of this are shown in Fig. 3. In each case, the brazed seal region remains entirely intact. The average strength of the 600 μm thick bilayers is 187 ± 39 MPa, as measured at room temperature using ball-on-ring biaxial flexure testing (ASTM F 394-78). The corresponding range of rupture strength values, indicated by the shaded regions in Fig. 2(a) and (b), are the effective pressures at which failure is expected to occur in the cell; i.e. the type of failure observed in Fig. 3. To verify this, additional testing was conducted using the 1200 μm thick bilayer discs. Specimens in the as-joined and the 200 and 800 h aging (in air) conditions displayed no leaking or failure through either the seal or cell out to the maximum rupture test pressure of 130 psi.

As a point of comparison, rupture strength data obtained on barium aluminosilicate (BAS)-based glass sealed speci-

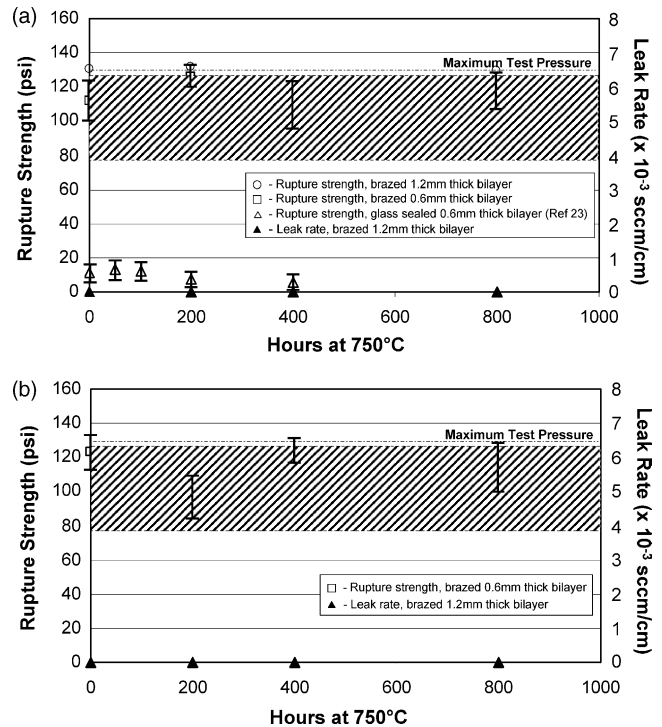


Fig. 2. Leak rate and rupture strength of the bilayer/Ag<sub>4</sub>CuO/Crofer-22 APU specimens as a function of exposure time in: (a) 750 °C air and (b) 750 °C wet hydrogen.

mens (from Ref. [23]) are also included in Fig. 2(a). Note that the thermal aging of glass seals in air leads to a degradation in seal strength. Two reasons for this phenomenon were offered: (1) the microstructure and composition of the glass-ceramic in the bulk portion of the sealing glass changes with time at temperature and (2) the reaction zone that forms at the glass/metal interface during initial sealing also evolves during soaking at high temperature. In both cases, the coefficient of thermal expansion (CTE) of the resulting ma-



Fig. 3. Examples of specimen failure upon rupture testing.



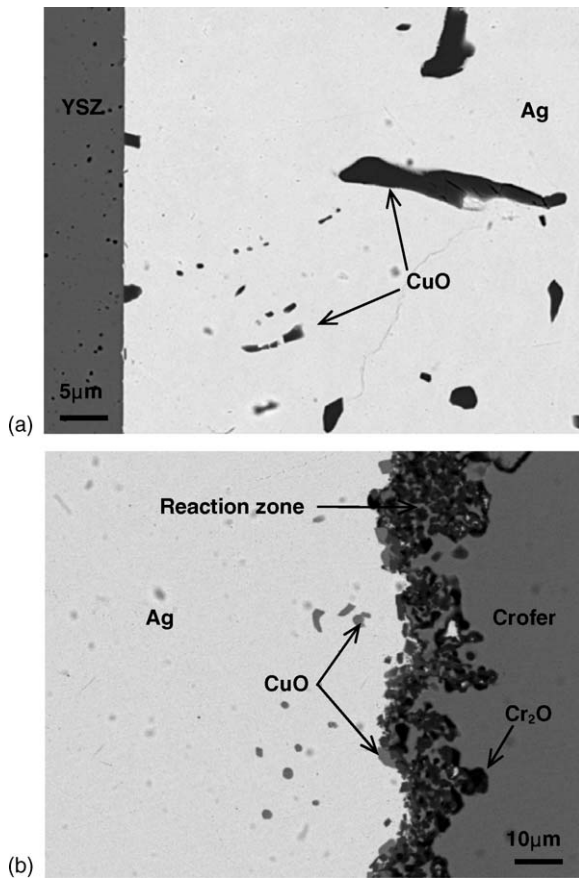


Fig. 4. Cross-sectional SEM micrographs of an as-joined rupture specimen: (a) along the YSZ–braze interface and (b) along the braze–Crofer interface.

terial that forms in the bulk of the seal and at the interfaces decreases relative to the original as-joined state. Thus upon cooling to room temperature, large thermally induced mismatch stresses are generated in the sealing material and the substrates, which subsequently causes a reduction in the measured rupture strength. In contrast, although the brazed seals also experience substantial CTE mismatch upon cooling ( $\alpha_{\text{bilayer}} \sim 11.2 \times 10^{-6} \text{ K}^{-1}$ ,  $\alpha_{\text{Crofer}} \sim 12.5 \times 10^{-6} \text{ K}^{-1}$ , and  $\alpha_{\text{silver}} \sim 22.8 \times 10^{-6} \text{ K}^{-1}$ ), the ductile sealing material yields and plastically deforms, thereby mitigating the transfer of significant stresses to the adjacent substrates. It is likely that the mechanical properties of the silver, i.e. low yield strength and high elongation, are instrumental in allowing the brazed seals to remain intact.

Shown respectively in Figs. 4 and 5 are typical cross-sectional micrographs of two specimens, one in the as-brazed condition and the other after aging in  $750^\circ\text{C}$  air for 400 h. A comparison of the YSZ–braze and braze–Crofer interfaces in each indicates that this exposure condition has little effect on the bulk or interfacial microstructures of the brazed seal. As seen in Fig. 4(a), the silver-based braze wets the YSZ substrate quite well, infiltrating into the submicron roughness along the interface. EDX analysis gave no indication of a reaction zone at the YSZ–braze interface, although a

dispersion of half-lens shaped CuO crystallites along this interface were readily observed, with essentially pure silver in between. Additional CuO precipitates are found in the bulk portion of the filler metal. The composition of the surrounding matrix is again elemental silver. As shown in Fig. 5(a), this interfacial microstructure is retained in the aged sample. Microstructural analysis conducted on the other specimens aged in  $750^\circ\text{C}$  air gave similar results.

On the Crofer side of the as-brazed joint, shown in Fig. 4(b), the interface between the braze and the underlying metal substrate assumes an undulating morphology. Seen as dark patches adjacent to the metal in Fig. 4(b), chromia scale doped with iron and manganese oxide forms on the Crofer. Some of the chromia reacts with the copper oxide in the braze, leading to the development of a  $\sim 10\ \mu\text{m}$  thick reaction zone. EDX analysis indicates that the reaction product consists of two phases: (1) a copper chromate phase with a composition that approximates  $\text{CuCr}_2\text{O}_4$  and (2) a mixed oxide containing both CuO and  $\text{Cr}_2\text{O}_3$  in apparent solid solution. Examination of the corresponding micrograph for the air exposed specimen in Fig. 5(b) suggests that no significant microstructural changes occur along the braze–Crofer interface during isothermal aging. The thickness and composition of the reaction zone and underlying oxide scale remain con-

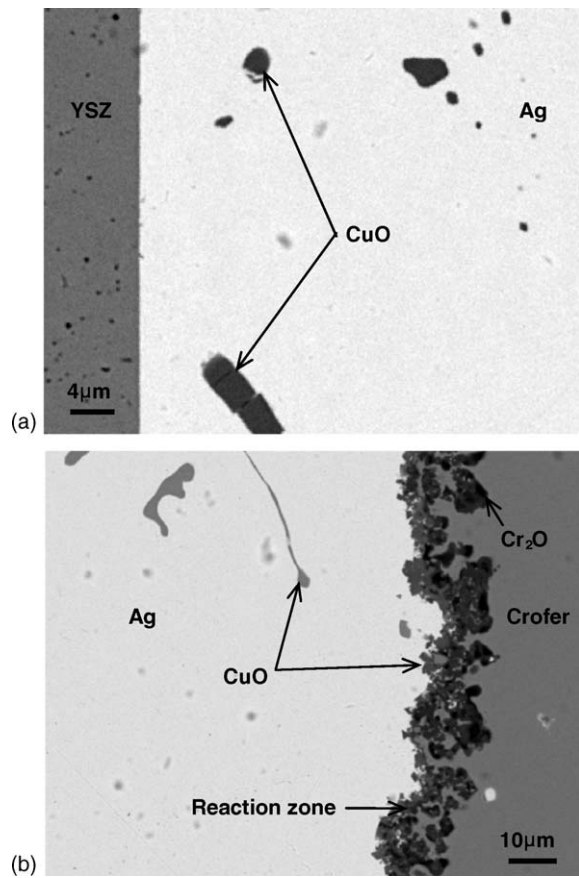


Fig. 5. Cross-sectional SEM micrographs of a rupture specimen that was exposed at  $750^\circ\text{C}$  to air ( $20\ \text{cm}^3\ \text{min}^{-1}$ ) for 400 h: (a) along the YSZ–braze interface and (b) along the braze–Crofer interface.

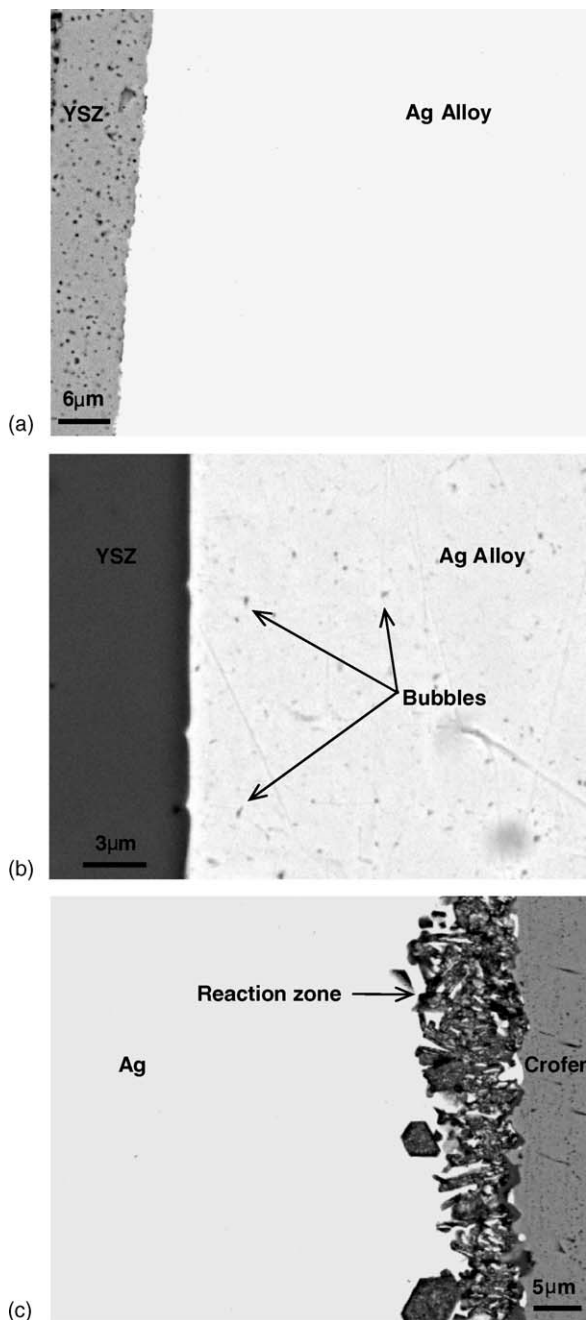
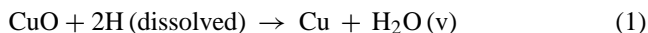


Fig. 6. Cross-sectional SEM micrographs of a rupture specimen that was exposed at 750 °C to wet hydrogen ( $10 \text{ cm}^3 \text{ min}^{-1}$ ) for 200 h: (a) along the YSZ–braze interface, (b) at higher magnification along the YSZ–braze interface, and (c) along the braze–Crofer interface.

stant. Measurements of the distance between the YSZ and the scale on the Crofer in these two samples indicate that the braze region is approximately 100  $\mu\text{m}$  thick.

Noticeable changes in the braze microstructure were observed in the samples that were aged in wet hydrogen, as seen by comparing the micrographs in Fig. 6 with the corresponding micrographs in Fig. 4. Within 200 h of exposure at 750 °C, the CuO particles in the filler metal appear to have reduced to metallic copper, Fig. 6(a), which subsequently alloys with

the adjacent silver matrix. EDX analyses of representative regions in this specimen indicate that the copper content in the filler material has essentially homogenized, with an average composition of 3.4 at.% Cu in Ag measured. As shown in the high magnification image of the YSZ–braze interface in Fig. 6(b), the reduction process is accompanied by the formation of porosity. That is, hydrogen diffuses into the Ag-based filler metal simultaneously causing reduction of the CuO and formation of water vapor presumably by



Since water vapor is not soluble in the silver, it precipitates as a gas-filled bubble. As seen in Fig. 6(b), the bubbles are widely dispersed and are submicron in size. Given the relatively high solubility and diffusion rate of hydrogen in silver at 750 °C [25] the presence of internal reduction is not surprising. Longer term exposure appears to cause an increase in the size of the bubbles up to an average size of  $\sim 0.5 \mu\text{m}$  after 800 h of exposure accompanied by a decrease in their number, suggesting that coarsening occurs. In all cases observed in the present study, the concentration of bubbles remains far below that required for percolation and therefore does not lead to a potential leak path.

As seen in Fig. 6(c), the reduction phenomenon extends to the Crofer side of the joint. Again, the lack of CuO precipitates in the matrix or along the reaction zone with the Crofer scale indicates that it reduces completely to copper and subsequently dissolves into the surrounding silver. The apparent ingress of silver alloy well into the reaction zone suggests that the CuO in the mixed CuO–Cr<sub>2</sub>O<sub>3</sub> reaction product reduces as well and thereby provides a pathway for the solid-state diffusion of silver. On the other hand, the copper chromate appears to remain stable and is the remaining constituent in the reaction zone. As noted previously, the hydrogen-aged specimens failed in the same manner as those aged in air, i.e. within the ceramic bilayer, which indicates that the membrane remains the weakest component in the sealing system. Given the microstructural changes that occur in the hydrogen-aged specimen, we speculate that if the braze filler region was isolated from the rest of the system, measurable degradation in joint strength relative to comparable as-brazed and air-aged joints would be observed. Efforts to carry out this measurement using a torsion testing technique are currently underway. However from an engineering design standpoint, it is apparent that the microstructural evolution which takes place in the seal does not cause a shift in the mode of failure nor does it lead to a loss in hermeticity or effective strength.

### 3.2. Effects of thermal cycling

Plotted in Fig. 7 are the average leak rates and rupture strengths of the thermally cycled sealing specimens as a function of the number of cycles to which the specimens

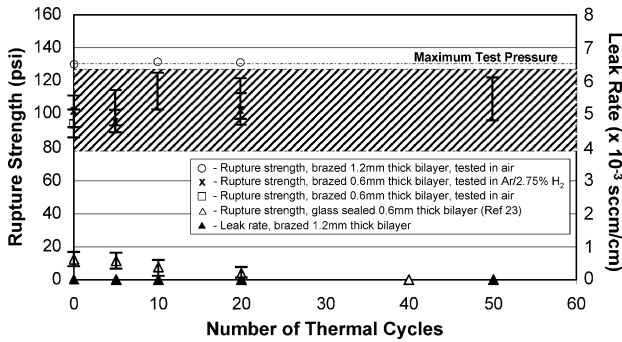


Fig. 7. Leak rate and rupture strength of the bilayer/Ag4CuO/Crofer-22 APU specimens as a function of the number of thermal cycles between room temperature and 750 °C.

were exposed. The results indicate that rapid thermal cycling causes no measurable degradation in either hermeticity or rupture strength. As with the aging specimens, all of the thermally cycled specimens exhibit rupture strengths that fall within the failure band for the 0.6 mm thick bilayer material. This finding appears to be independent of the test atmosphere; i.e. in either Ar/2.75% H<sub>2</sub> or air. All of these specimens also fail in the same manner, through the ceramic bilayer membrane, indicating that this remains the weakest component in the brazed seal upon thermal cycling. This was again verified by re-testing using specimens that contain 1.2 mm thick bilayers. Samples of this type that were exposed to 0, 10, and 20 thermal cycles in air could all be rupture tested to the maximum pressure of 130 psi without failure.

Comparison with previous tests conducted on BAS glass sealed specimens, included in Fig. 7, indicates that the brazed seals do not suffer from the type of degradation observed in the glass seals. The glass joints experience a substantial loss in strength beyond ten thermal cycles. Again, this phenomenon is attributed to compositional/microstructural changes in the bulk glass and the interfacial reaction zone with the Crofer that give rise to mismatch stresses along the glass/substrate interfaces during cooling. Unlike what is suspected to occur in the Ag-based braze seal, these stresses cannot be mitigated via strain relaxation mechanisms associated with yielding but instead reduce the effective stress that the seal is able to withstand.

Shown in Fig. 8 are a series of SEM micrographs that display the YSZ–braze interface in specimens that have undergone 5, 10, and 50 rapid thermal cycles. These can be compared with the same interface in the as-brazed specimen shown in Fig. 4(a). Examination reveals that after 5 and 10 thermal cycles, Fig. 8(a) and (b) respectively no significant change in interfacial microstructure occurs. However after 50 cycles, Fig. 8(c), signs of delamination along the YSZ–braze interface appear. Small patches, ~5–20 μm in length, are observed where the braze has pulled away from the YSZ to form a thin void. As was found with pore formation in the H<sub>2</sub>-aged samples, the practical effect of this

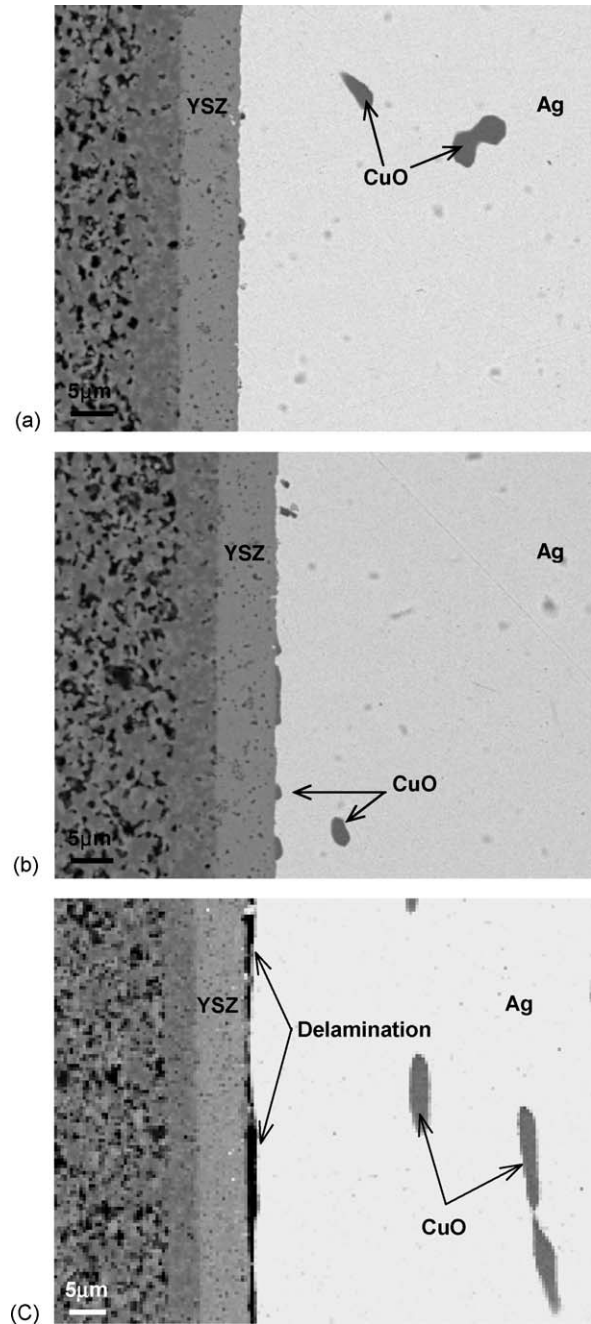


Fig. 8. Cross-sectional SEM micrographs of the YSZ–braze interfaces within three rupture specimens that were thermally cycled in air at 75 °C min<sup>-1</sup> between room temperature and 750 °C: (a) for 5 cycles, (b) for 10 cycles, and (c) for 50 cycles.

phenomenon on rupture strength and mode of specimen failure under pressurization is essentially nil, i.e. the strength of the ceramic membrane remains the dominant factor in defining failure in the partially delaminated seals. However in an effort to identify the operational limit for thermal cycling in this type of seal, testing will continue to determine the point at which rupture strength degradation is eventually observed.



#### 4. Summary and conclusion

This series of initial experiments to examine the effects of high-temperature exposure and thermal cycling on air-brazed seals revealed the following:

- 1 The braze microstructure appears to remain constant in 750 °C air out to 800 h of isothermal exposure. However, exposure to wet hydrogen causes the internal CuO precipitates in the filler metal to reduce to copper metal, which is accompanied by the precipitation of water vapor bubbles. Complete reduction occurs within 200 h of exposure at 750 °C. With additional exposure time, the microstructure of the reduced filler appears to coarsen. The reduced copper dissolves into the silver, but there is no subsequent loss in adhesion with either of the adjoining substrates.
- 2 Although microstructural changes take place in the hydrogen exposed specimens, rupture testing demonstrates no loss in hermeticity or any measurable change in rupture strength. In comparison with the as-joined specimens, the aged rupture test joints statistically display the same strength regardless of exposure atmosphere or aging time, out to 800 h. The mode of specimen failure remains constant regardless of the test conditions; i.e. via fracture through the bilayer membrane.
- 3 Specimens that were thermally cycled at 75 °C min<sup>-1</sup> showed little change in microstructure out to 10 cycles. However after 50 cycles, signs of delamination along the YSZ–braze interface were present.
- 4 Subsequent rupture testing indicates that no accompanying degradation in rupture strength takes place. The ceramic membrane remains the weakest constituent in the seal. Both this behavior and that of the aging specimens stand in stark contrast with comparably conditioned glass seal specimens, which display severe joint strength degradation with both aging and thermal cycling. Based on these results, more extensive exposure and thermal cycle testing is underway to determine the long-term limitations of air-brazed seals for potential application in SOFC stacks.

#### Acknowledgments

The authors would like to thank Nat Saenz, Shelly Carlson, and Jim Coleman for their assistance in sectioning and polishing the popgun samples and conducting the metallographic and SEM analysis work. This work was supported

by the U.S. Department of Energy, Office of Fossil Energy, Advanced Research and Technology Development Program. The Pacific Northwest National Laboratory is operated by Battelle Memorial Institute for the United States Department of Energy (U.S. DOE) under Contract DE-AC06-76RLO 1830.

#### References

- [1] B.C.H. Steele, A. Heinzl, *Nature* 414 (2001) 345.
- [2] S.-B. Sohn, S.-Y. Choi, G.-H. Kim, H.-S. Song, G.-D. Kim, *J. Am. Ceram. Soc.* 87 (2004) 254.
- [3] K. Eichler, G. Solow, P. Otschik, W. Schaffrath, *J. Eur. Ceram. Soc.* 19 (1999) 1101.
- [4] K.D. Meinhardt, J.D. Vienna, T.R. Armstrong, L.R. Pederson, U.S. Patent No. 6,430,966 (2001).
- [5] S.-B. Sohn, S.-Y. Choi, G.-H. Kim, H.-S. Song, G.-D. Kim, *J. Non-Cryst. Sol.* 297 (2002) 103.
- [6] S.P. Simner, J.W. Stevenson, *J. Power Sources* 102 (2001) 310.
- [7] Y.-S. Chou, J.W. Stevenson, L.A. Chick, *J. Am. Ceram. Soc.* 86 (2003) 1003.
- [8] J. Duquette, A. Petric, *J. Power Sources* 137 (2004) 71.
- [9] C.A. Lewinsohn, S. Elangovan, *Ceramic Engineering and Science Proceedings*, vol. 24, American Ceramic Society, 2003, p. 317.
- [10] A.K. Jadoon, *J. Mater. Sci.* 39 (2004) 593.
- [11] J. Intrater, *Mater. Manuf. Proc.* 8 (1993) 353.
- [12] J. Mei, P. Xiao, *Scripta Mater.* 40 (1999) 587.
- [13] T.I. Khan, A. Al-Badri, *J. Mater. Sci.* 38 (2003) 2483.
- [14] C.W. Fox, G.M. Slaughter, *Welding J.* 43 (1964) 591.
- [15] F. Barbier, C. Peytour, A. Revcolevschi, *J. Am. Ceram. Soc.* 73 (1990) 1582.
- [16] K.S. Weil, J.Y. Kim, J.S. Hardy, *Electrochem. Sol. Stat. Lett.* 8 (2005) A133.
- [17] J.S. Hardy, J.Y. Kim, K.S. Weil, *J. Electrochem. Soc.* 151 (2004) J43.
- [18] J.Y. Kim, J.S. Hardy, K.S. Weil, *J. Am. Ceram. Soc.*, in press.
- [19] S. Mukerjee, C. De Minco, *Proceedings of the First International Conference on Fuel Cell Science Engineering and Technology*, American Society of Mechanical Engineers, 2003, p. 507.
- [20] P. Lamp, J. Tachtler, O. Finkenwirth, S. Mukerjee, S. Shaffer, *Fuel Cells* 3 (2003) 146.
- [21] S.P. Simner, J.F. Bonnett, N.L. Canfield, K.D. Meinhardt, J.P. Shelton, V.L. Sprenkle, J.W. Stevenson, *J. Power Sources* 113 (2003) 1.
- [22] K.S. Weil, C.A. Coyle, J.Y. Kim, J.S. Hardy, *Materials Research Society Symposium Proceedings*, vol. 756, Materials Research Society, 2003, p. 551.
- [23] K.S. Weil, J.E. Deibler, J.S. Hardy, D.S. Kim, G.-G. Xia, L.A. Chick, C.A. Coyle, *J. Mater. Perform.* 13 (2004) 316.
- [24] G.P. Anderson, S.J. Bennett, K.L. De Vries, *Analysis and Testing of Adhesive Bonds*, Academic Press, 1977.
- [25] V.N. Verbetsky, S.V. Mitrokhin, *Diff. Defect Data Part B: Sol. Stat. Phenom.* 73 (2000) 503.